Original Article

SHM Structural Health Monitoring

Structural Health Monitoring
2023, Vol. 22(3) 1601–1612

DOI: 10.1177/14759217221112451
journals.sagepub.com/home/shm
SAGE

An information fusion approach for increased reliability of condition monitoring With homogeneous and heterogeneous sensor systems

Vigneshwar Kannan, Dzung Viet Dao and Huaizhong Li

Abstract

In machinery condition monitoring, it is often vital to consider information from multiple sources due to possible sensor failure or signal distortion, which may result in misclassification of the health status. An issue with multiple sensor data fusion, however, is that the classification can be affected by conflicting results between sensor signals. The proposed method uses a novel three-module approach to information fusion in order to address the problem. Features corresponding to signal integrity are extracted and employed for training a one-class support vector machine to detect unwanted distortions or sensor failures. Different classifiers are trained for the different sensor types available and each signal recorded is used to determine machine health. Decision-level fusion is conducted through a majority voting system using the integrity scores derived from the OCSVMs and the separate classification results. From this, a dynamically weighted fault diagnosis based on sensor signal quality is obtained. Experimental verification using vibration and acoustic emission signals show that the framework is viable and allows for an increased reliability in machinery health diagnosis.

Keywords

condition monitoring, information fusion, vibration, acoustic emission, multisensor system, signal integrity

Introduction

Traditional condition monitoring of rotational machinery typically focuses on a single sensor monitoring approach. Although this has led to great success, existing methods could greatly benefit through the use of information fusion also known as data fusion. Information fusion is the process of combining information from multiple sensors or sources with the aim of achieving an output of a higher accuracy or reliability.[1] Information fusion is often divided into three main classes, namely data-level, feature-level and decision-level fusion.[2]

Data-level fusion directly combines the raw signals acquired from sensors in order to generate information rich data. This allows for a high accuracy. However, this level of fusion retains the largest amount of information in comparison to the other types, making real time processing a difficult task. Wang et al.[3] used accelerometers for multisensor fault diagnosis by firstly converting signals into a combined representation in the form of an image. A bottleneck layer optimised convolutional neural network (CNN) was used for feature extraction and classification of faults in machinery. Similarly, Xia et al.[4] combined accelerometer signals at the data-level as a two-dimensional matrix and used CNN for rotating machinery fault diagnosis. Jing et al.[5] used a data sample that consisted of signal segments from various sensor types as input to a deep CNN. This allowed for the diagnosis of planetary gearbox faults.

Feature-level fusion allows the various features to first be extracted from each signal using appropriate signal processing techniques. The extracted features are then combined at this level to obtain relevant information. Chen and Li[6] employed time and frequency domain features extracted from accelerometers positioned in different locations of machinery. Features were fused with multiple two-layer sparse autoencoders and used as inputs to a deep belief network for bearing fault classification. Tao et al.[7]

School of Engineering and Built Environment, Gold Coast Campus, Griffith University, Southport, QLD, Australia

Corresponding author:
Huaizhong Li, School of Engineering and Built Environment, Gold Coast Campus, Griffith University, Southport, QLD 4222, Australia.
Email: h.li@griffith.edu.au

diagnosed bearing faults with multiple vibration signals through the use of a deep belief network. Characteristics extracted were used to generate a suitable classifier for diagnosis using multiple sensors. Vanraj et al.[8] performed classification of gear conditions with features extracted from microphone and accelerometer signals through various methods. A float forward selection algorithm was utilised to determine relevant features to be used with a k-nearest neighbour for diagnosis.

In decision-level fusion, the highest level of information fusion, decisions on classification are first made individually on each sensor available. The local decisions for each sensor are then fused to obtain an overall classification on the state of the machinery. Niu et al.[9] made use of both current and vibration signals for motor fault diagnosis. Separate classifiers were employed for each signal, then decisions were combined with multi-agent classifier fusion algorithm. Safizadeh and Latifi[10] utilised load cells and accelerometers for bearing health monitoring as each of the sensors performed better in different cases. The waterfall fusion process model was used for decision-level fusion. Zhong et al.[11] conducted fault diagnosis of an automotive engine by also taking advantage of decision level fusion. Classifications were obtained individually from various sensors and were combined through a probabilistic ensemble method.

Many researchers have incorporated information fusion to obtain a higher reliability for the diagnosis of defects for multi-sensor systems. Although it is common to conduct information fusion on the same type of sensors, condition monitoring systems can also benefit through the use of different sensor types.[12] A system using the same type of sensors is often referred to as homogeneous sensor system, while a system using different types of sensors is referred to as heterogeneous sensor system. Various types of sensors present advantages in different scenarios. The combination of the information available can increase the overall accuracy and reliability of fault diagnosis. Of the different condition monitoring methods that exist, vibration-based monitoring is quite common and has been researched extensively. It utilises accelerometers appropriately positioned to detect mechanical oscillation of components of a machine about an equilibrium encountered during operation.[13] Signals can be processed, and relevant features are extracted to determine the presence of a machine fault. Another common monitoring method is using acoustic emission (AE). Acoustic emission signals, like acceleration signals, can also be analysed in the time-domain, frequency-domain, or time-frequency domain for the detection of various features related to the machine condition. Studies have recognised AE for its ability to detect incipient defects, and its performance is better than accelerometers in low speed operating conditions for fault diagnosis.[14–16] Li et al.[17] proposed a method for gearbox fault diagnosis through the simultaneous use of vibration and AE signals. Deep Boltzmann machines were used for each set of statistical parameters derived from wavelet packet transform of each of the sensors. Random forest was then used on the deep representation of features from both sensors to obtain a fused classification output. Although such approaches have been able to achieve more reliable condition monitoring, the possibility of sensor issues and its impact on the diagnosis has rarely been discussed.

Oftentimes, studies work under the assumption that signals obtained from sensors are of good quality. However, this is not always the case. Training data can be carefully selected through visual inspection to reflect the behaviour of good quality signals for diagnosis. Unfortunately, sensor signals in realistic applications can be corrupted or distorted and affect classification accuracy. Mey et al.[18] proposed a method where vibration and AE data from transducers were used in separate multi-layer perceptrons. Activations were applied at a combined classifier. This method also allowed for fault detection in cases where a sensor provided unreliable monitoring data due to sensor failure. In addition to sensor failure, it is also important to consider issues that may compromise the integrity of signals. Girondin et al.[19] mentioned that sensor related issues can impact time and frequency domain of data obtained. Their study involved the detection of accelerometer loosening which is a common issue in helicopter health usage and monitoring systems. Abboud et al.[20] also acknowledged that sensor issues can have a drastic effect on the waveform of signals causing misleading diagnoses. The effects of accelerometer detachment were investigated and a symmetry-based indicator for its detection was developed. Similarly, Randall and Smith[21] proposed a method for the detection of faulty mounting of accelerometers as it can affect measurement validity. Although such studies exist, signal integrity has not been considered in the context of information fusion for machinery condition monitoring to the best of the authors' knowledge. In a multisensor data fusion review presented by Khaleghi et al.,[22] the many challenges of fusion were briefly discussed. This included imperfections in the measurement and conflicting results in fusion. Reducing the effects of data imperfections and accounting for conflicting results are vital in ensuring the reliability of condition monitoring systems.

This paper aims to create a multisensor fusion framework that can be adapted for both homogeneous and heterogeneous sensor systems to increase overall accuracy and reliability of classification. Testing will be conducted on a bearing fault diagnosis application using both accelerometers and an AE sensor for monitoring. The proposed method will identify signals that could potentially be distorted affecting features extracted and reduce its influence on the overall classification result. This is accomplished by assigning a dynamic weight to individual sensor

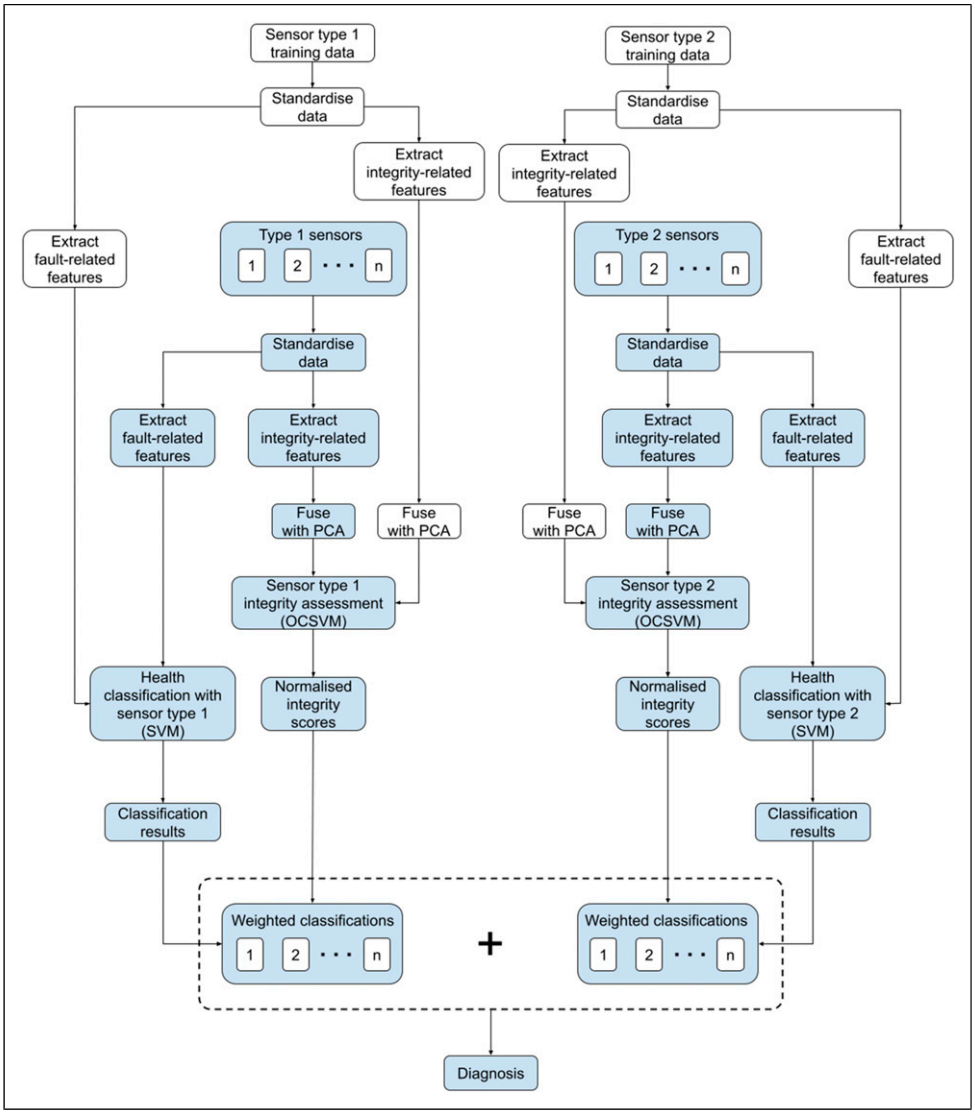

Figure 1. Proposed architecture for dynamically weighted multisensor machine health classification based on signal integrity using different sensor types.

classifications based on signal integrity prior to decision-level fusion so as to achieve a more reliable output. The robustness of the approach is verified through testing for bearing health with different sensor issues affecting measurement.

Methodology

The architecture of the proposed approach can be divided into three modules, namely, signal integrity, fault diagnosis and decision-level fusion. This section will give a detailed explanation on the development of each module and also the experimental setup used for verification on a bearing fault simulator. Figure 1 illustrates the generalised framework of the proposed method where white blocks indicate the training process with training data, and the blue blocks indicate the diagnosis process of sensor input. Testing involves firstly extracting relevant feature sets from standardised signal input. Integrity-related features are fused with principal component analysis (PCA) before being used as input to the integrity assessment classifier. A normalised integrity score is obtained from each sensor signal. Similarly, fault-related features are used as input to the health classifier for a fault diagnosis. Each sensor's diagnosis is then assigned a weightage which is the corresponding signal integrity score calculated. The health condition can then be identified by determining which class has the highest aggregate integrity score. The MATLAB programming language was used for the implementation of the proposed method along with the statistics and machine learning

toolbox. Nevertheless, the approach can be recreated in whichever programming language suitable.

The implementation of the approach uses accelerometers and an AE sensor. However, the method should be applicable to other sensor types producing a similar temporal signal as long as appropriate fault-related features are used for analysis. The use of more sensors should generally yield a higher reliability as integrity issues faced may only affect an individual sensor or a sensor type while others remain unaffected.

Signal integrity assessment

It has been known that sensor related issues affect the vibration signals and the information extracted from them. Studies in the area have focused on the detection of a particular issue such as faulty sensor mounting,[21] detachment,[20] and loosening.[19] Although such methods do prove to be successful for what is being detected, it may be more practical to implement an anomaly detection method capable of distinguishing any signal abnormality from what is considered normal behaviour for a system. For this, one-class support vector machines (OCSVMs) were implemented for each sensor type. This was achieved through the use of selected features pertaining to signal anomalies for training the algorithm. Prior to extraction of features, the signals were divided by the standard deviation for standardisation purpose. The features extracted were the arithmetic mean, the first quartile, the second quartile (median) and the third quartile as shown in equations (1) to (4), respectively

$$\mu = \frac{1}{n}\sum_{i=1}^{n} x_i \tag{1}$$

$$Q_1 = \frac{x(n+1)}{4} \tag{2}$$

$$Q_2 = \frac{x(n+1)}{2} \tag{3}$$

$$Q_3 = \frac{x3(n+1)}{4} \tag{4}$$

Here n is the number of values and x is the dataset in ascending order. It should be noted that the equations shown for quartile calculations are common approximations only and that statistical packages are able to calculate this to a higher accuracy. The dimensionality of the feature set was then reduced through PCA. From this, the principal components showing the highest variance were selected for training purpose. This was achieved by computing the covariance matrix as shown in equation (5)

$$A = \begin{bmatrix} Cov(\mu,\mu) & Cov(\mu,Q_1) & Cov(\mu,Q_2) & Cov(\mu,Q_3) \\ Cov(Q_1,\mu) & Cov(Q_1,Q_1) & Cov(Q_1,Q_2) & Cov(Q_1,Q_3) \\ Cov(Q_2,\mu) & Cov(Q_2,Q_1) & Cov(Q_2,Q_2) & Cov(Q_2,Q_3) \\ Cov(Q_3,\mu) & Cov(Q_3,Q_1) & Cov(Q_3,Q_2) & Cov(Q_3,Q_3) \end{bmatrix} \tag{5}$$

Each element of the matrix involved computing the covariance for each combination of features using

$$Cov(a,b) = \frac{\sum_{i=1}^{n}(a_i - \overline{a})(b_i - \overline{b})}{n} \tag{6}$$

where a_i and b_i are the values of the two features from 1 to n, and $\overline{a}$ and $\overline{b}$ are the mean of the features. Given the covariance matrix (A), the eigenvalues (λ) and matrix of eigenvectors (v) that satisfy equation (7) were determined

$$Av = \lambda v \tag{7}$$

The eigenvectors were then ranked according to the magnitude of eigenvalues to obtain the order of principal components from highest to lowest variance. Most of the variance in the data from the original features can typically be represented with the highest principal components alone while others can be omitted. An in-depth overview of the PCA technique was given by Abdi and Williams.[23] The training data were then converted into this alternative representation by multiplying with the selected eigenvectors before being used in the OCSVM. It must be noted that upon testing, the features extracted from samples are also to be converted into the same feature space where the training data for the sensor type was previously used. The OCSVM works by training a support vector machine (SVM) with a feature set from a single class of data. This includes signals with conditions reflective of good and bad machine health without sensor abnormalities so that any sensor issues manifesting itself in the signal can be recognised. In order to distinguish anomalies, the OCSVM finds a hyperplane that maximises the separation between training data and the origin. Equation (8) presents the OCSVM classifier's objective function such that $(w \cdot \phi(X_i)) \geq \rho - \xi_i$ and $\xi_i \geq 0$

$$\min_{w,\xi_i,\rho} \frac{1}{2}\|w\|^2 + \frac{1}{vn}\sum_{i=1}^{n}\xi_i - \rho \tag{8}$$

Here ϕ is the feature map, w is a weight vector, ξ_i is the slack variable, ρ is an offset and v is the upper limit on training data that are outliers and lower limit on the data used as support vectors.[24] The kernel function, radial basis function, was used to project data into a higher dimensional space and as shown

$$K(X_1, X_2) = e^{-\gamma \|X_1 - X_2\|^2} \tag{9}$$

where γ denotes the scaling parameter and X_1 and X_2 are points in space plotted against the selected principal components. Typically, a hyperplane is formed by solving the minimisation problem with Lagrange multipliers (α_i) to obtain a decision function as seen in equation (10)

$$f(X) = sgn((w \cdot \phi(X)) - \rho) = sgn\left(\sum_{i=1}^{n} \alpha_i K(X_i, X) - \rho\right) \tag{10}$$

As a soft margin was used in the OCSVM allowing for a more generalised model, the occurrence of misclassifications near the hyperplane were expected. This was addressed by assigning an integrity score to classifications that fall near the margin. Although such an approach for a single sensor will not be of much use, a multisensor system can utilise the score to assign an appropriate weightage to predictions from the sensor array. This was accomplished by removing the signum function from the decision function in equation (10) and censoring outputs exceeding a set positive and negative threshold denoted by t as shown in equation (11)

$$I = \begin{cases} -t, & (w \cdot \phi(X)) - \rho < -t \\ +t, & (w \cdot \phi(X)) - \rho > +t \\ (w \cdot \phi(X)) - \rho, & \text{otherwise} \end{cases} \tag{11}$$

This threshold may be any value that accurately represents the range in which the decision function output is unreliable making the signal integrity score (I) limited to $-t \leq I \leq +t$. The integrity score obtained was then normalised between 0 and 1 as shown

$$\widehat{I} = \frac{I + t}{2t} \tag{12}$$

where $\widehat{I}$ denotes the normalised integrity scores. The signal is considered to be of poor quality when the score is 0 and good when it is 1. For cases in between, the signal may have an issue but could potentially still be misclassified.

Fault diagnosis

Numerous studies have been conducted identifying signal features corresponding to the presence of defects in machinery. These features are often used with machine learning techniques in order to distinguish the different health conditions that may occur during operation. The proposed method employed SVMs for the classification of faults. This was accomplished by using various features from the time and frequency domain for training the models. The time domain features used were kurtosis (K), root mean square (RMS), crest factor (CF) and skewness (S) as shown in equations (13) to (16), respectively

$$K = \frac{\sum_{i=1}^{n} (x_i - \mu)^4}{n\sigma^4} \tag{13}$$

$$RMS = \sqrt{\frac{1}{n} \sum_{i=1}^{n} x_i^2} \tag{14}$$

$$CF = \frac{\max|x_i|}{\sqrt{\frac{1}{n}\sum_{i=1}^{n} x_i^2}} \tag{15}$$

$$S = \frac{\sum_{i=1}^{n} (x_i - \mu)^3}{n\sigma^3} \tag{16}$$

where μ is the mean and σ is the standard deviation.[25] Kurtosis has been identified as a good indicator of bearing health as healthy bearings have a Gaussian amplitude distribution with a kurtosis value of 3 regardless of speed or loading conditions.[26] A faulty bearing compared to one that is in good condition has a higher RMS value which can be expected to increase with the development of the fault.[27] The impact caused by the contact of the defect to the raceway or rolling elements can be calculated using the crest factor. The change in the pattern of vibration on signals due to this defect is reflected in the increase of this feature's magnitude.[28] The asymmetry of the vibration signal is measured using skewness to tell if it is negatively or positively skewed.[29] Bearings in a healthy operating condition have signals with near-zero skewness. Although these features have previously been used to provide insight on the variation of health condition in machinery, they were not quite as good in diagnosing the fault type.

In addition to the time domain features, more features were extracted from the envelope spectrum. Envelope analysis is a technique that is used to separate defect related frequency components from the signal through band demodulation.[30] This allows for the periodic impulse related frequencies such as bearing defects to be visualised on the envelope spectrum. The frequency of the bearing defects coming into contact with other moving components can be calculated using geometrical parameters and operational speed. Equations, (17), (18) and (19) show the ball pass frequency of the outer race $(BPFO)$, ball pass frequency of the inner race $(BPFI)$ and the ball spin frequency (BSF), respectively[31]

$$BPFO = \frac{nf_r}{2}\left(1 - \frac{d}{D}\cos\theta\right) \tag{17}$$

$$BPFI = \frac{nf_r}{2}\left(1 + \frac{d}{D}\cos\theta\right) \tag{18}$$

$$BSF = \frac{Df_r}{2d}\left(1 - \left(\frac{d}{D}\cos\theta\right)^2\right) \tag{19}$$

Here f_r is the operational frequency, θ is the contact angle, n is the number of rolling elements, D is the pitch diameter and d is the rolling element diameter of the bearing. It can be assumed that a certain defect is present when prominent peaks or their harmonics align with a calculated defect frequency. To use this information for training, a demodulation band optimal to its respective sensor type was chosen and the envelope spectrum was obtained. As the ball spin frequency corresponds to the ball defect's contact with only one of the two races, it was multiplied by two. The amplitude at each of the defect frequencies were then divided by the RMS of the spectrum to obtain a normalised representation of the features. For fault diagnosis, a separate SVM model was trained for each sensor type with its respective signal features as the behaviour of features would be expected to vary. When testing simultaneously recorded signals, a classification would be obtained for each sensor used. Support vector machines segregate data points of two classes through the use of a hyperplane in a higher dimensional space in order to create a non-linear decision boundary.[32] Equation (20) shows the SVM classifier's objective function such that $y_i(w^T\phi(x_i) + b) \geq 1 - \xi_i$ and $\xi_i \geq 0$

$$\min_{w,b,\xi_i} \frac{\|w\|^2}{2} + C\sum_{i=1}^{n}\xi_i \tag{20}$$

where b is the bias and C is a constant relating to margin width and the number of data points within it. Solving the minimisation problem, the decision function in equation (21) is obtained

$$f(X) = sgn\left(\sum_{i=1}^{n}\alpha_i y_i K(X_i, X) + b\right) \tag{21}$$

Cortes and Vapnik[32] provide a detailed explanation on SVM. Originally, the machine learning technique was developed for the classification of two groups. It has since been applied for multi-class problems through the use of one-versus-one or one-versus-rest approaches.[33] Therefore, it can be applied to the diagnosis of bearing health conditions.

Decision-level fusion

Decision-level fusion can allow for a higher reliability in diagnosing machine health than with single sensor monitoring. However, conflicting diagnoses can make it difficult to determine the health condition and maintenance actions required. Unlike many common decision-level fusion approaches that simply focus on combining multiple classifications, a weighted aggregation was performed depending on the sensor integrity determined. This is akin to the fusion implemented in ensemble classification methods known as majority voting. In majority voting, the output from each classifier is considered as a vote for the respective class.[34] The total number of votes for each class are aggregated and the class with the majority is selected as the output. The drawback of such a method is that the signal used to obtain a classification may not be of good quality potentially affecting the determined class. This was overcome by taking into consideration the normalised integrity scores of each sensor as shown

$$C_x = \sum_{i=1}^{n} c_i \widehat{I}_i \tag{22}$$

where C_x represents the aggregate normalised integrity score for a possible class from the classifiers, c is a binary value dependant on if the sensor predicted class corresponds with C_x, $\widehat{I}$ is the normalised signal integrity score and n is the number of sensors used regardless of sensor type. For n sensors used, the magnitude of C_x can range from 0 to n. Equation (23) shows that the fused classification of sensors (C_f) can be computed by identifying the class with the highest aggregate integrity score

$$C_f = \max\{C_1, C_2, \ldots, C_n\} \tag{23}$$

This class represents the overall predicted classification for the condition monitoring system.

Experimental setup

Validation of the proposed method was accomplished with the SpectraQuest Machinery Fault Simulator-Lite as shown in Figure 2. The left bearing housing was used to hold Rexnord ER12KCL ball bearings of varying health conditions, namely, healthy, outer race fault (ORF), inner race fault (IRF) and ball fault (BF). Specifications of the bearing used are given in Table 1.

The training set used a triaxial accelerometer and an AE sensor positioned on the fault simulator as illustrated in Figure 2. The triaxial accelerometer was a PCB Piezotronics model 356A16 with sensitivities of 9.43, 9.83 and 9.81 mV/(m/s^2) on the X, Y and Z axes, respectively, and the AE sensor was a Kistler 8152B221 with a sensitivity of 48 dBref 1 V/(m/s). The machine was operated at various shaft frequencies for healthy bearing conditions and two faulty bearing conditions with different defect sizes. Multiple measurements were recorded from the sensors using an ECON AVANT MI-7008 dynamic signal analyser. Samples for training and testing were collected at a sampling frequency of 96 kHz for one second as a trade-off between signal information captured and computational speed. A

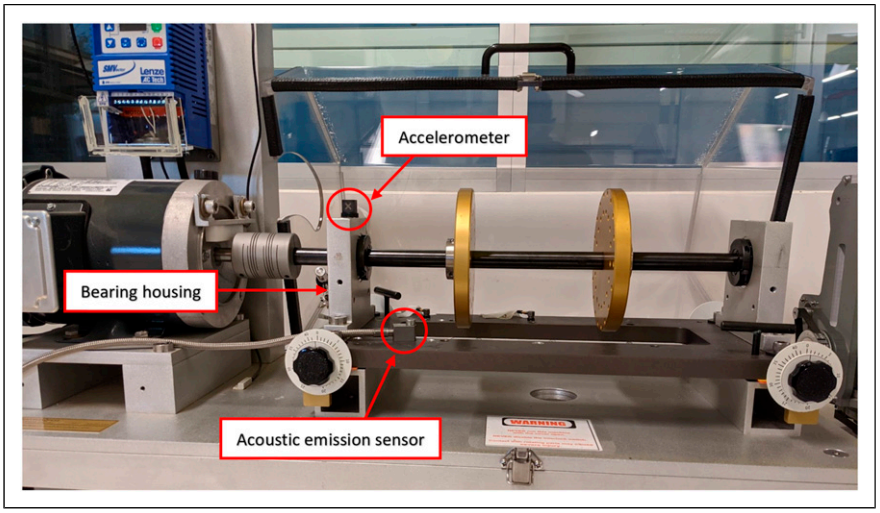

Figure 2. SpectraQuest machinery fault simulator-lite used for collection of vibration and AE signals.

Table 1. Rexnord ER12KCL bearing specifications.

Pitch diameter (mm)	Rolling element diameter (mm)	Number of rolling elements	Contact angle (degrees)
33.5	7.938	8	0

total of 480 training samples were used for the accelerometer classifier collected from all three axes of the vibration sensor. The AE classifier also had 480 samples collected for training purpose. All training samples were recorded at shaft frequencies of 17, 27, 37 and 47 Hz. The testing dataset used to validate the proposed approach was collected from the fault simulator after taking apart and reassembling components with the same sensors reattached in roughly the same positions. This will show whether the method is robust to the natural variations in signal characteristics that can be expected to occur with a typical monitoring scenario. Data were collected from shaft frequencies of 17, 27, 37 and 47 Hz with 160 different recording samples from each sensor recorded simultaneously. Table 2 shows the number of samples used by each sensor for training and testing purposes.

The training dataset contained accelerometer and AE signals of a normal quality only whereas the testing dataset included both normal quality signals and signals subjected to sensor related issues. The issues induced were different levels of saturation on the accelerometer and disconnected power supply on the AE sensor. Table 3 shows information on the number of signals with integrity issues for each sensor included in the testing dataset. This can be used to verify the accuracy of signal anomalies detected. The PC used to run the proposed method on MATLAB had 8 GB RAM and an i5-1035G7 CPU.

Results and discussion

Prior to diagnosis of the testing dataset, three individual vibration signals were analysed to validate the use of the signal integrity and fault diagnosis module. The three individual signals and its respective histograms are shown in Figure 3. Table 4 shows the features used to determine the integrity scores where cases A, B and C correspond to signals in Figure 3(a)–(c), respectively. It can be noted that case A and B have a mean value near zero. Similarly, the first and third quartiles are roughly equidistant from the second quartile for both the cases. Although these distances themselves may vary, the features are standardised accounting for changes in magnitude. However, due to the saturation found in case C, the signal with bearing defect is negatively skewed. This causes the mean and second quartile to be shifted negatively. Furthermore, the first and third quartile are not equidistant from the second quartile. The module gives normalised integrity scores of 0.81, 1 and 0 for cases A, B and C, respectively. Although case A had a score slightly less than 1, it could be attributed to the signal falling close to the hyperplane generated but is still high enough to be considered good quality. This shows that the four features can be used to effectively distinguish signals that are considerably different to what the signal integrity model is trained on. In the fault diagnosis module, cases A, B and C were predicted as Healthy, ORF and BF, respectively. Both cases with good quality signals were accurately predicted but the case with a saturated signal was misclassified. As the normalised integrity score found for case C was 0, its prediction will carry no influence on the fused prediction when using multiple sensors.

The total time taken to train the models for signal integrity and classification using the training dataset was about 209 s. Classification using the proposed approach on

Table 2. Signal information used for training and testing datasets.

Sensor Type	Sensor and mounting orientation	Samples per class	
		Training dataset	Testing dataset
Accelerometer	PCB piezotronics 356A16 (X-axis)	40	40
	PCB piezotronics 356A16 (Y-axis)	40	40
	PCB piezotronics 356A16 (Z-axis)	40	40
Acoustic emission	Kistler 8152B221 (Y-axis)	120	40

Table 3. Number of signals with integrity issues from testing dataset.

Sensor	BF	Healthy	IRF	ORF
Accelerometer (X-axis)	0	0	0	0
Accelerometer (Y-axis)	0	0	1	10
Accelerometer (Z-axis)	0	0	0	20
Acoustic emission	10	0	10	0

monitoring through a one-second interval processing manner. Thus, the time delay between the fault occurrence and diagnosis would be less than one second. The results for the testing dataset are shown as follows. The data were used to generate a confusion matrix for each of the sensors available in Figure 4, showing the number of samples with signal integrity issues present (class −1) and those of good quality (class 1). Note that for illustrative purposes, class −1

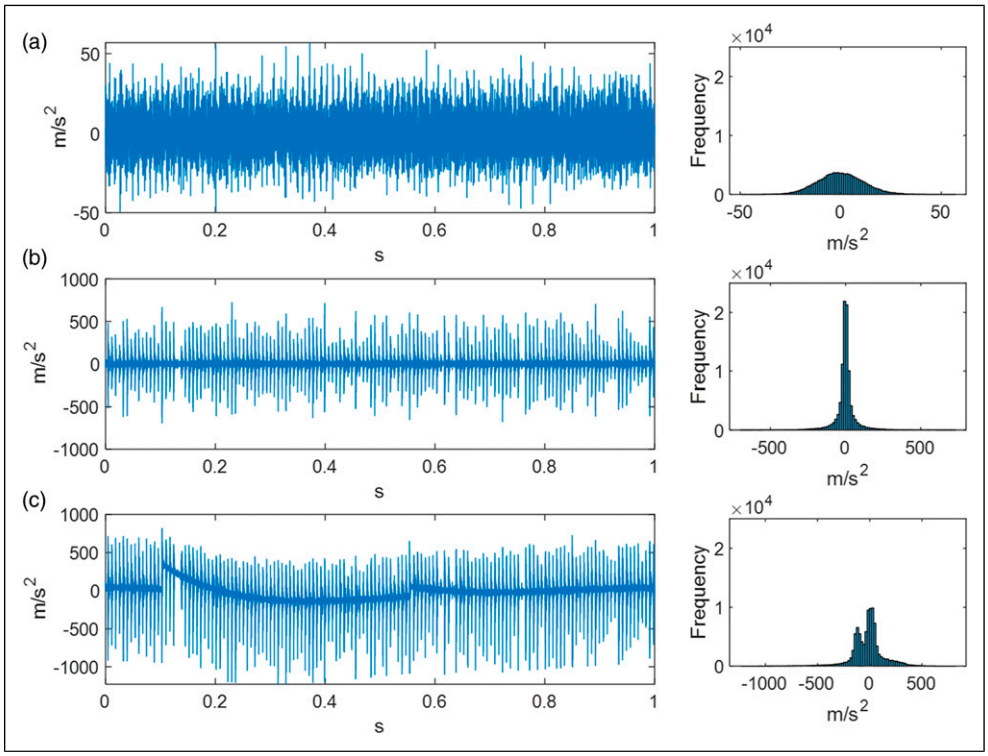

Figure 3. Vibration signal and its respective histogram for (a) healthy bearing with good quality signal, (b) outer race fault (ORF) bearing with good quality signal and (c) outer race fault bearing with saturated signal.

the 160 samples from the testing dataset, each including a one second signal from every sensor used, took about 153 s in total. This means that one second of monitoring all sensors used is processed for classification in less than a second. With the PC specifications and sensors employed, the method can theoretically be utilised for real-time online

not only includes signals that had a normalised integrity score of 0 but also any that had a score of less than 1 where it was not absolutely certain whether quality was affected. In the X-axis of the accelerometer, most signals were correctly classified as good quality except two samples. The Y-axis accelerometer had assigned lower scores to six good quality

Table 4. Calculated features for signal integrity module for the signals illustrated in Figure 3.

Features	Case A	Case B	Case C
μ	0	−0.07	−22.60
Q_1	−7.60	−16.77	−102.26
Q_2	−0.25	−0.10	−10.60
Q_3	7.45	16.37	39.89

As observed in Figure 5, the accuracy of the X-axis, Y-axis and Z-axis accelerometer signals are 95, 93.75 and 86.25%, respectively. Although the misclassifications in the X-axis accelerometer can be attributed to the model being trained on limited data per class, most Y-axis accelerometer misclassifications correspond to samples with low signal integrity. Although signals from the Z-axis accelerometer are also subjected to signal distortion, the misclassifications

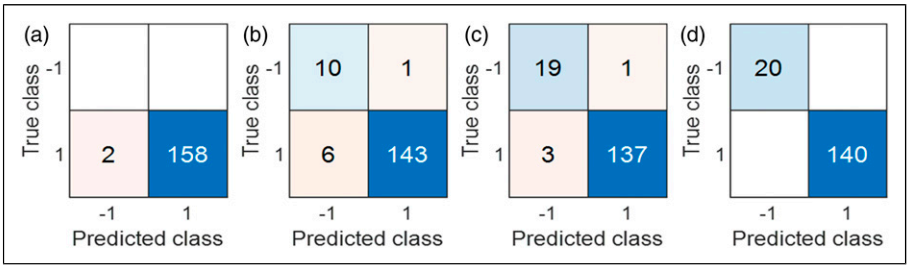

Figure 4. Signal integrity confusion matrix for (a) X-axis accelerometer, (b) Y-axis accelerometer, (c) Z-axis accelerometer and (d) AE sensor.

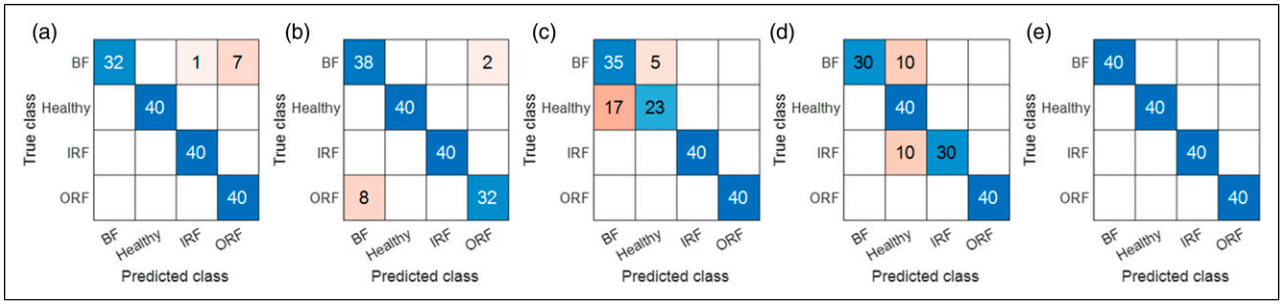

Figure 5. Fault classification confusion matrix of (a) X-axis accelerometer, (b) Y-axis accelerometer, (c) Z-axis accelerometer, (d) AE sensor and (e) fused classification output.

signals and also misclassified one of low quality. Similarly, of the Z-axis accelerometer signals, three were assigned low normalised integrity scores while being of acceptable quality and one sample with integrity issues was misclassified. For the AE sensor, all signals were correctly classified. The signal output for the AE sensor can be easily distinguished as the waveform is significantly different when the power supply is disconnected. The baseline shift in vibration signals due to accelerometer saturation can be more ambiguous due to different levels of saturation present. Despite this, the confusion matrices show that the proposed method is able to assign integrity scores accurately for almost all cases.

The classification results obtained from each of the sensors along with the fused output on the testing dataset is shown in Figure 5 in the form of confusion matrices. Note that the signals from each sensor used to obtain each fused output were all recorded simultaneously.

do not correspond with classes that have integrity issues. Therefore, accuracy was likely hindered due to the limited training dataset. The AE on the other hand misclassifies all signals with integrity issues and no others while still being trained on a small dataset. It can be seen that some classifiers perform better than others in certain scenarios, but the occurrence of signal integrity issues further reduces the accuracy. Using the proposed method, taking into consideration each of the sensor signals and their normalised integrity scores, a 100% accuracy has been achieved in this case as shown in Figure 5(e).

This does not necessarily mean that the proposed method can always be accurate. Rather, it proves that it is capable of exploiting multisensor information for reliable diagnosis by accounting for potential signal issues that may affect the integrity of the prediction. Integrity issues encountered with any individual sensor does not typically impact the accuracy of predictions from other sensors. The use of various sensor

types also proves to be advantageous as certain issues affecting signal integrity, and in turn classification accuracy, will not affect all sensor types. This can be seen in the case of accelerometer signal saturation causing distortions. Although the high vibrations due to certain operating conditions may cause most accelerometer signals to be distorted, alternative signal types such as the AE remains unaffected. If the classification output was fused without accounting for signal integrity, prediction results would be biased by the accelerometers despite possibly being inaccurate. The proposed approach is able to account for these signal issues effectively and achieve a relatively high accuracy in comparison to individual sensors. Of course, it would be unreasonable to expect the fused performance of the classification method to perform better than each individual signal in every case. Cases can still be encountered where the signals have a good integrity, but an error occurs due to misclassification. This could lead to two classes being equally likely to have occurred according to the approach. With the use of more training data from a range of operating conditions, classification accuracy of each model can be further improved. Similarly, using more sensor types will increase the reliability of the proposed approach. This, in turn, will increase the overall classification accuracy but also increase the complexity of the approach and the computational burden.

The proposed method, in comparison to other information fusion approaches, has the advantage of being able to reduce or omit a sensor's influence from negatively affecting the overall classification of the multisensor system. A similar study exists in which a heterogenous multisensor system is capable of diagnosing machine condition even in the event of sensor failure.[18] The method involved a combination of classifiers which could still produce a diagnosis from the other working sensor. The study does mention that their developed algorithm is not capable of distinguishing when either one of the sensors used is more reliable. In the case of signal distortions, unlike sensor failure, information is still being fed to the algorithm which could potentially affect the overall classification accuracy. This is where the proposed method excels as it takes signal integrity of sensors into consideration in the diagnosis process. This allows for a more robust fault diagnosis approach that is able to produce reliable results.

Conclusion

In realistic applications of multisensor condition monitoring systems, sensors used are susceptible to various integrity issues. These issues manifest themselves in the form of distortions in signals. Despite the use of multisensor systems to improve reliability of classification, the integrity of each sensor is not often considered which could severely affect the condition determined. The paper presents a novel approach to efficiently utilise homogeneous and heterogeneous sensor information through dynamically assigning each a weightage dependant on signal quality. This is achieved through the use of the anomaly detection models for each sensor type trained on a representation of features pertaining to good signal quality. Through this method, an integrity score can be dynamically assigned to data depending on its perceived signal quality. A classifier for each sensor type is then used to obtain a fault diagnosis output for each sensor. Each decision is weighted in accordance with the normalised signal integrity score obtained and fused to achieve a more reliable classification prediction. The proposed method was validated using different sensors mounted on a fault simulator to determine the bearing health condition. The classification accuracy of individual sensors being hindered due to sensor issues and a limited dataset for training of the classifier was overcome by the proposed approach allowing for an increased reliability and accuracy.

Declaration of Conflicting Interests

The author(s) declared no potential conflicts of interest with respect to the research, authorship, and/or publication of this article.

Funding

The author(s) received no financial support for the research, authorship, and/or publication of this article.

ORCID iDs

Vigneshwar Kannan https://orcid.org/0000-0002-5353-3308
Huaizhong Li https://orcid.org/0000-0002-5617-702X

References

1. Castanedo F. A review of data fusion techniques. *Sci World J* 2013; 2013: 1–19.
2. Duan Z, Wu T, Guo S, et al. Development and trend of condition monitoring and fault diagnosis of multi-sensors information fusion for rolling bearings: a review. *Int J Adv Manuf Technol* 2018; 96: 803–819.
3. Wang H, Li S, Song L, et al. A novel convolutional neural network based fault recognition method via image fusion of multi-vibration-signals. *Comput Ind* 2019; 105: 182–190.
4. Xia M, Li T, Xu L, et al. Fault diagnosis for rotating machinery using multiple sensors and convolutional neural networks. *IEEE/ASME Trans Mechatronics* 2018; 23(1): 101–110.
5. Jing L, Wang T, Zhao M, et al. An adaptive multi-sensor data fusion method based on deep convolutional neural networks

for fault diagnosis of planetary gearbox. *Sensors (Switzerland)* 2017; 17(2): 414.
6. Chen Z and Li W. Multisensor feature fusion for bearing fault diagnosis using sparse autoencoder and deep belief network. *IEEE Trans Instrum Meas* 2017; 66(7): 1693–1702.
7. Tao J, Liu Y and Yang D. Bearing fault diagnosis based on deep belief network and multisensor information fusion. *Shock Vib* 2016; 2016: 1–9.
8. Vanraj, Dhami SS and Pabla BS. Hybrid data fusion approach for fault diagnosis of fixed-axis gearbox. *Struct Heal Monit* 2018; 17(4): 936–945.
9. Niu G, Han T, Yang BS, et al. Multi-agent decision fusion for motor fault diagnosis. *Mech Syst Signal Process*. 2007; 21(3): 1285–1299.
10. Safizadeh MS and Latifi SK. Using multi-sensor data fusion for vibration fault diagnosis of rolling element bearings by accelerometer and load cell. *Inf Fusion* 2014; 18: 1–8.
11. Zhong JH, Wong PK and Yang ZX. Fault diagnosis of rotating machinery based on multiple probabilistic classifiers. *Mech Syst Signal Process* 2018; 108: 99–114.
12. Li X, Wan S, Liu S, et al. Bearing fault diagnosis method based on attention mechanism and multilayer fusion network. *ISA Trans*. 2021. In Press.
13. Measuring Vibration with Accelerometers [Internet]. National Instruments. Available from: http://www.ni.com/en-au/innovations/white-papers/06/measuring-vibration-with-accelerometers.html. (2020, accessed 15 August 2020
14. Elforjani M and Mba D. Accelerated natural fault diagnosis in slow speed bearings with Acoustic Emission. *Eng Fract Mech* 2010; 77(1): 112–127.
15. Eftekharnejad B, Carrasco MR, Charnley B, et al. The application of spectral kurtosis on acoustic emission and vibrations from a defective bearing. *Mech Syst Signal Process* 2011; 25(1): 266–284.
16. Van Hecke B, Yoon J and He D. Low speed bearing fault diagnosis using acoustic emission sensors. *Appl Acoust* 2016; 105: 35–44.
17. Li C, Sanchez RV, Zurita G, et al. Gearbox fault diagnosis based on deep random forest fusion of acoustic and vibratory signals. *Mech Syst Signal Process* 2016; 76–77: 283–293.
18. Mey O, Schneider A, Enge-Rosenblatt O, et al. Condition monitoring of drive trains by data fusion of acoustic emission and vibration sensors†. *Processes* 2021; 9(7): 1–13.
19. Girondin V, Loudahi M, Morel H, et al. Vibration-based fault detection of accelerometers in helicopters. *IFAC Proc Volumes (IFAC-PapersOnline)* 2012: 45: 720–725. Elsevier
20. Abboud D, Elbadaoui M, Becquerelle S, et al. Detection of sensor detachment in aircraft engines using vibration signals. In: Cavalca KL and Weber HI (eds) *Proceedings of the 10th International Conference on Rotor Dynamics -- IFToMM*. Cham: Springer International Publishing, 2019. p. 351–365.
21. Randall RB and Smith WA. Detection of faulty accelerometer mounting from response measurements. *J Sound Vib* 2020; 477: 115318.
22. Khaleghi B, Khamis A, Karray FO, et al. Multisensor data fusion: a review of the state-of-the-art. *Inf Fusion* 2013; 14(1): 28–44.
23. Abdi H and Williams LJ. Principal component analysis. *Wiley Interdiscip Rev Comput Stat* 2010; 2: 433–459. John Wiley & Sons, Ltd.
24. Schölkopf B, Williamson R, Smola A, et al. Support vector method for novelty detection. *Adv Neural Inf Process Syst* 2000; 14: 582–588.
25. Mollasalehi E. *Data-driven and model-based bearing fault analysis - wind turbine application*. Unpublished doctoral thesis. Calgary, AB: University of Calgary, 2017.
26. Dyer D and Stewart RM. Detection of rolling element bearing damage by statistical vibration analysis. *Am Soc Mech Eng* 1977; 100(2): 229–235.
27. Shen Z, He Z, Chen X, et al. A monotonic degradation assessment index of rolling bearings using fuzzy support vector data description and running time. *Sensors (Switzerland)* 2012; 12(8): 10109–10135.
28. Tom KF. *A primer on vibrational ball bearing feature generation for prognostics and diagnostics algorithms*. Army Research Lab. Adelphi; 2015. https://apps.dtic.mil/sti/citations/ADA614145
29. Caesarendra W and Tjahjowidodo T. A review of feature extraction methods in vibration-based condition monitoring and its application for degradation trend estimation of low-speed slew bearing. *Machines* 2017; 5(4): 21.
30. Kannan V, Li H and Dao DV. Demodulation band optimization in envelope analysis for fault diagnosis of rolling element bearings using a real-coded genetic algorithm. *IEEE Access* 2019; 7: 168828–168838.
31. Mais J. *Spectrum analysis: the key features of analyzing spectra*. SKF USA, Inc. 2002. https://www.skf.com/binaries/pub12/Images/0901d1968024acef-CM5118-EN-Spectrum-Analysis_tcm_12-113997.pdf
32. Cortes C and Vapnik V. Support-vector networks. *Mach Learn* 1995; 20(3): 273–297.
33. Bishop CM. *Pattern recognition and machine learning*. New York: Springer, 2006.
34. Bramer M. *Principles of data mining*. 3rd ed. London: Springer London, 2016. (Undergraduate Topics in Computer Science).

Appendix

Pseudocode for the generalised framework proposed.

```
% Training
For number of sensor types available for monitoring
      Standardise training data of good quality signals under different machine health
      conditions
      Extract features relating to signal integrity and machine health from standardised
      data
      Use PCA to dimensionally reduce integrity-related features
      Train OCSVM with integrity features from that sensor type
      Train SVM with fault-related features from that sensor type
End
% Testing
For machine monitoring period
      For number of sensors available for monitoring
            Standardise signal obtained from sensor
            Extract features from standardised signal
            Use PCA to dimensionally reduce integrity-related features from sensor data
            Input integrity-related features from sensor to respective OCSVM model
            Output normalised signal integrity score from respective OCSVM
            Input fault-related features from sensor to respective SVM model
            Output machine health condition from respective SVM
      End
      Aggregate normalised integrity scores of sensors for each health condition
      Compute condition with the largest aggregate score for diagnosis result
End
```